AGU ADVANCING EARTH AND SPACE SCIENCES

Earth's Future

RESEARCH ARTICLE

10.1029/2025EF006095

Key Points:

- The study introduces the severe water scarcity (SWS) indicator as proxy for the soil moisture in rainfed grain production worldwide
- The study indicates the existence of a significant relationship between the SWS-affected area and the global wheat price
- The agricultural area affected by SWS will increase under future climate resulting in higher estimated wheat price levels

Supporting Information:

Supporting Information may be found in the online version of this article.

Correspondence to:

M. Trnka,
trnka.m@czechglobe.cz

Citation:

Trnka, M., Meitner, J., Balek, J., Feng, S., Gaviria, J. A., Fischer, M., et al. (2026). Climate-induced severe water scarcity events as harbingers of global wheat price. *Earth's Future*, *14*, e2025EF006095. https://doi.org/10.1029/2025EF006095

Received 6 FEB 2025
Accepted 10 JUL 2026

Author Contributions:

Conceptualization: Miroslav Trnka, Song Feng, Petr Havlík, Gabriel Katul, Jørgen E. Olesen
Investigation: Miroslav Trnka, Jan Meitner, Jan Balek, Milan Fischer, Petr Havlík, Kurt-Christian Kersebaum, Claas Nendel, Margarita Ruiz-Ramos, Markéta Poděbradská, Ulf Büntgen, Zdeněk Žalud
Methodology: Miroslav Trnka, Jan Meitner, Jan Balek, Song Feng, Juliana Arbelaez Gaviria, Milan Fischer, Esther Boere, Daniela Semerádová, Max Torbenson
Supervision: Mikhail A. Semenov, Jan Esper, Gabriel Katul, Jørgen E. Olesen

Climate-Induced Severe Water Scarcity Events as Harbingers of Global Wheat Price

Miroslav Trnka[1,2], Jan Meitner[1,2], Jan Balek[1,2], Song Feng[3], Juliana Arbelaez Gaviria[1,2,4], Milan Fischer[1,2], Esther Boere[4,5], Petr Havlík[4], Kurt-Christian Kersebaum[1,6,7], Claas Nendel[6,8], Margarita Ruiz-Ramos[9], Daniela Semerádová[1,2], Mikhail A. Semenov[10], Markéta Poděbradská[1,2], Jan Esper[1,11], Ulf Büntgen[1,12,13], Max Torbenson[11], Jáchym Brzezina[1], Zdeněk Žalud[1,2], Gabriel Katul[1,14], and Jørgen E. Olesen[1,15,16]

[1]Global Change Research Institute CAS, Brno, Czech Republic, [2]Department of Agrosystems and Bioclimatology, Mendel University in Brno, Brno, Czech Republic, [3]Department of Geosciences, University of Arkansas, Fayetteville, AR, USA, [4]International Institute for Applied Systems Analysis (IIASA), Laxenburg, Austria, [5]Vrije Universiteit, VU University Amsterdam, Amsterdam, The Netherlands, [6]Leibniz Centre for Agricultural Landscape Research (ZALF), Müncheberg, Germany, [7]Georg August University, Göttingen, Germany, [8]University of Potsdam, Institute of Biochemistry and Biology, Potsdam, Germany, [9]CEIGRAM-Research Centre for the Management of Agricultural and Environmental Risks, Universidad Politécnica de Madrid, Madrid, Spain, [10]Rothamsted Research, Harpenden, UK, [11]Department of Geography, Johannes Gutenberg University, Mainz, Germany, [12]Department of Geography, University of Cambridge, Cambridge, UK, [13]Swiss Federal Research Institute WSL, Birmensdorf, Switzerland, [14]Department of Civil and Environmental Engineering, Duke University, Durham, NC, USA, [15]Department of Agroecology, Aarhus University, Tjele, Denmark, [16]iCLIMATE Interdisciplinary Centre for Climate Change, Aarhus University, Roskilde, Denmark

Abstract This study connects the dots between global extent of severe water scarcity (SWS) events and spikes in food price. The authors start with three staple crops (rice, wheat, and maize) using a empirical but crop specific characterization of severe water scarcity occurrence, which is defined based on the area of land cultivated with each studied crop that on a given year is under SWS conditions. Water scarcity is estimated based on 1, 3, and 12 months standardized precipitation evapotranspiration index during crop specific sensitive periods (SPs). SPs coincide with the 4 months prior to harvest. A SWS-wheat price relationship model was developed for period 2001–2021 and tested for 1986–2000 and 2022–2024 with future projections calculated under climate change using climate model simulations from CMIP5 and CMIP6 up to 2100. The results show a marked increase in wheat prices driven by increasing SWS area, which is in turn a function of greenhouse gas emissions. The results indicate that the meanglobal mean temperature increase by 3°C (compared to 1951–1980) could lead to the tripling of the mean global wheat price compared to 2010 (after deflating).

Plain Language Summary Water scarcity is a growing threat to global food production, particularly for crops that depend on rainfall rather than irrigation. When soils do not receive enough moisture during key growing periods, harvests can fail, and food prices can rise. In this study, we introduce a new way to track severe water scarcity (SWS) by measuring the area of cropland affected during sensitive stages of crop growth. We apply this method to major staple crops and examine how changes in SWS are associated with global food prices. We find a clear link between the area affected by severe water scarcity and global wheat prices. Years with larger affected areas tend to coincide with higher prices. Looking ahead, climate model projections suggest that water scarcity will expand under continued warming. Our results indicate that a temperature increase of about 3°C could triple average global wheat prices relative to 2010. These findings highlight the risks climate change poses to global food security and the consequences of more frequent water shortages in agriculture.

1. Introduction

Wheat, maize, and rice account for 42% of the global societal dietary energy supply and 37% of the global protein supply (Figure 1a) (FAO, 2022). Wheat is the main source of protein for humans (19%), and rice and wheat combined constitute the dominant sources of calories (37% each) (FAO, 2022). Thus, the prominence of cereals in the global food system is not in dispute; the sheer scale of cereal production and land use underscores this point (Figure 1). Wheat, rice and maize account for 51% of the global blue water footprint (i.e., fresh surface and groundwater use) (Mekonnen & Hoekstra, 2011), and in addition wheat has the largest rainfed area of the three

Visualization: Jan Meitner, Jan Balek, Juliana Arbelaez Gaviria, Daniela Semerádová, Jáchym Brzezina
Writing – original draft: Miroslav Trnka, Jan Meitner, Juliana Arbelaez Gaviria, Markéta Poděbradská, Ulf Büntgen, Max Torbenson, Gabriel Katul
Writing – review & editing: Miroslav Trnka, Jan Meitner, Jan Balek, Song Feng, Juliana Arbelaez Gaviria, Milan Fischer, Esther Boere, Petr Havlík, Kurt-Christian Kersebaum, Claas Nendel, Margarita Ruiz-Ramos, Daniela Semerádová, Mikhail A. Semenov, Markéta Poděbradská, Jan Esper, Ulf Büntgen, Max Torbenson, Jáchym Brzezina, Zdeněk Žalud, Gabriel Katul, Jørgen E. Olesen

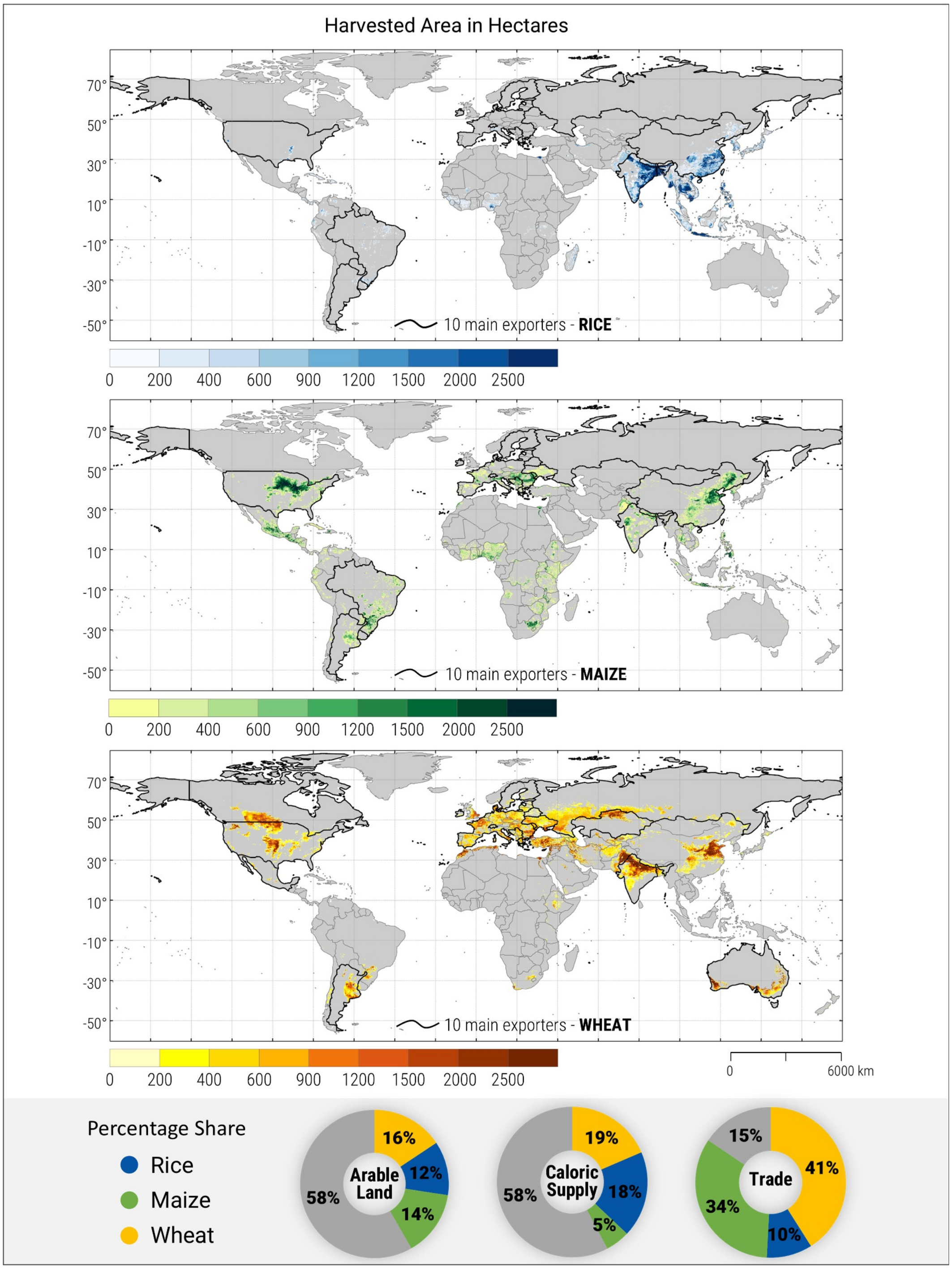

Figure 1. Main areas of rice/maize/wheat production with the borders of the 10 top exporting countries highlighted. The donut charts indicate the shares of the three major crops in the global arable land area, calorie supply and agricultural commodity trade.

major cereals (Portmann et al., 2010). Any change in water availability (or lack thereof) will therefore likely impact these crops' production, availability, and price.

Approximately 14% of global cereal production is traded internationally, with 90% of these exports generated by the top 10 producing countries. While wheat, maize, and rice production has steadily increased over the past 60 years, the prices of these cereals showed a marginal overall increase between 1960 and 2000, followed by significant increases over the past 24 years. Among the three crops, wheat is a particularly volatile commodity (Conceição & Mendoza, 2009) exhibiting punctuated growth. During the grain price crises of 2007/08, 2010/11 and 2021/22, wheat prices increased by 97%, 46%, 64%, respectively, relative to the preceding years of increased prices. In comparison, rice prices changed by 124%, 2%, and −4%, respectively, and maize prices changed by 79%, 70%, and 66%, respectively in these years (IGC, 2022). Of far greater concern is the number of undernourished individuals. This number increased from 598 million in 2010 to 735 million by 2020 (FAO, 2022), an increase of 23% in 12 years.

By the middle of the century, the Food and Agriculture Organization (FAO) projected an increase of 40% in food and agricultural product demand compared with 2020 levels. Wheat is the most consumed cereal (0.6 Gt), and maize is the most consumed cereal as feed with 0.97 Gt (FAO, 2017). The necessary increases in agricultural output driven by this demand will likely be achieved by yield increases rather than cultivated land expansion. This change will primarily occur in emerging economies, presumably by improving various technologies and cultivation practices, including mobilizing production resources such as irrigation water and fertilizer (OECD & FAO, 2020). The challenge of maintaining a balance between cereal demand and supply under a changing climate is evident (Baker et al., 2018; Janssens et al., 2020; Zhu et al., 2022) with a particular concern raised regarding available water resources (Heinicke et al., 2022; Trnka et al., 2019).

The growing demand for cereals and price volatility are obviously only part of any future challenges to food security. Crop models predict 1.5%, 15.5%, and 6.7% decreases in global rice, maize, and wheat productivity levels, respectively, per 1°C of warming without adaptation (Hasegawa et al., 2022). These model projections of cereal productivity consider key factors such as long-term hydroclimatic changes, air temperature and vapor pressure deficit shifts, soil water conditions, irrigation, crop cultivar and management practices, and even the effects of increasing atmospheric CO_2 concentration levels on photosynthesis and water-use efficiency. The impacts of recurring climate patterns such as the El Niño–Southern Oscillation on heterogeneities in grain yields (Ubilava & Abdolrahimi, 2019) and prices (Ubilava, 2017, 2018) have also been studied. However most of these projections do not fully account for the occurrence of large-scale adverse climate extremes (Heinicke et al., 2022; Nendel et al., 2023) that can persist over extended durations coinciding with a particular crop growth stage. Although global warming is expected to increase the frequency of extreme events, the estimates of future agricultural commodity prices usually consider only long-term yield trends based on multiyear means (Hasegawa et al., 2018; Nelson et al., 2014). Thus, these projections not fully account for intensive, longer-lasting, large-scale or cooccurring water scarcity events (Hasegawa et al., 2022). The spatiotemporal relationships of such events and their compound impact on grain prices continue to be a formidable scientific challenge and a knowledge barrier and studies that attempt to deal with them (e.g., Mehrabi & Ramankutty, 2019 or Tigchelaar et al., 2018) do not consider the impact on prices.

To address these challenges, our work here seeks to bridge the influence of climate change along with its expected impact on water availability directly on cereal prices. We used the extent of severe water scarcity (SWS) defined as significant water balance anomaly in the sensitive period for the crop growth as a proxy for major water scarcity events. It was hypothesized that the relationship between global SWS extent and global cereal prices could be a predictor of the cereal price levels both in the given year and long-term. This would allow to estimate future cereal price levels from climate projections of SWS until 2050 and beyond. This study in its methodological framework considers not only SWS events in the given season but also impact of sequences of multiple SWSs on the global price level both in the recent past and the near future.

2. Materials and Methods

2.1. Severe Water Scarcity (SWS)

The concept of SWS events (Trnka et al., 2019), which combines three time scales of the standardized precipitation evapotranspiration index (SPEI) calculated using method described by Vicente-Serrano et al. (2010), is used here to specifically target the critical water shortage time frames for crop production (Table S1 in Supporting Information S1). An SWS event occurs when a negative soil moisture anomaly satisfies three conditions: (a) simultaneously persists during most of the growing season for a specific cereal, (b) peaks during the critical yield-forming period, and (c) occurs against the backdrop of a long-term water anomaly that generally reduces regional water resources (Table S1 in Supporting Information S1). The aggregation of SWS for cereal-growing areas allows accounting for all SWS events, as they occur across all cereal-growing areas simultaneously.

The areas of maize, rice and wheat production are unevenly distributed globally. However, well-defined production regions within global arable land are present (Figure 1) and can be further weighted by its productivity and access to irrigation (Figure S1 in Supporting Information S1). An increase in SWS events in key production regions may significantly increase the probability of experiencing SWS in key producing areas simultaneously (or nearly simultaneously), as has been shown in earlier case studies targeting wheat (Trnka et al., 2019). The primary advantage of the SWS concept is that it allows the likelihood of multiple rice–maize–wheat-producing areas experiencing spatio-temporally synchronized or/and sequenced SWS events to be analyzed, thus capturing simultaneous breadbasket shocks as described by Anderson et al. (2023). Across the whole globe and for each crop, the water scarcity occurrence over the 4 months preceding the typical local harvest date of the given crop was quantified. The probability of SWS events between 1861 and 2100 was based on the standardized precipitation evapotranspiration index (SPEI) calculated by the team. The SPEI accounts for both precipitation and potential evapotranspiration (PET) when assessing the onset and magnitude of a drought. A unified global 0.5° grid was used, and a given location within the grid was defined as an area affected by SWS event if both the short-term SPEI thought to impact the target crop production and the long-term SPEI presumably affecting the general water resource availability occurred in each grid cell. The levels of SPEI triggering SWS events are defined in the Table S1 in Supporting Information S1. The occurrence of SWS during the 1901–2021 period was first evaluated via the Climate Research Unit (CRU) data set (Harris et al., 2014), which represents "observed" SWS events. The annual SWS-affected area was subsequently considered a predictor of crop prices, and SWS–price models were subsequently developed and evaluated (Figure 2). The SWS probability was then estimated for the climate conditions provided by 31 global climate models (GCMs) from the sixth phase of the Coupled Model Intercomparison Project CMIP6 (Table S3 in Supporting Information S1). This was done both for the control climate period (1860–2014) and for climate projections (2015–2100). To provide more robust estimates of future climate, 27 GCMs from CMIP5 projects were also analyzed (Table S4 in Supporting Information S1). The SWS occurrence was examined under three shared socioeconomic pathways (SSPs) for CMIP6 (SSP1-2.6, 2-4.5 and 5-8.5) and corresponding representative concentration pathways or RCPs (RCP2.6, 4.5 and 8.5) in the case of CMIP5: (a) SSP1-2.6 and RCP2.6 correspond to the implementation of the 2015 Paris Agreement (26); (b) SSP2-4.5 and RCP4.5 correspond to the "average" pathway; and (c) SSP5-8.5 and RCP8.5 correspond to a high-emission world. This approach allowed us to estimate the effect of climate change mitigation on future grain price levels.

2.2. Crop Production Areas

The total arable land was considered, and SWS occurrences were determined for grids where the target crop is grown (Ramankutty et al., 2008) (i.e., maize, rice, and wheat grids—Figure S1 in Supporting Information S1). Weights were assigned to each grid according to the acreage of arable land, and each grid was then weighted based on its share of the total area of the target crop and held constant over the whole period. The areas of the individual crop grids constitute areas where the crops have been produced (Hoekstra et al., 2012). This area reached approximately 171 Mha for maize, 158 Mha for rice and 218 Mha for wheat (FAO, 2022). This approach facilitated estimates of how much of the global area for each crop was affected by SWS in each harvest year. Weighting the specific crop area allowed the effect of water scarcity changes on risk in the current primary production areas to be examined based on either the area or production. To analyze changes in the SWS patterns in the top exporting regions, the cumulative SWS probability in grids in the territories of the 10 most important exporters of each crop was examined over the 2010–2020 period, and the grids were weighted according to their share of the entire production area and the production quantity of each crop separately.

2.3. Price Data

The mean annual real world market wheat price as annual world market price for US hard red winter wheat, maize and rice (Thai 5%) from the Commodity Markets online database pink sheet of the World Bank were used. These prices are deflated and expressed in year 2010 US dollars (World Bank, 2025). Only the period from 1986 onwards was evaluated as global commodity trade was in general less globalized prior to the so-called Urugay round negotiations that started in 1986 and lead to World Trade Organization establishment in 1995. In addition International Grain Council (IGC, 2022) indices were considered since they capture prices in multiple shipment locations. This included the wheat price index (WPI) which is based on quotations of 10 varieties of wheat and different shipment locations, including Argentina, Australia, Canada, the US, and France. The maize price index

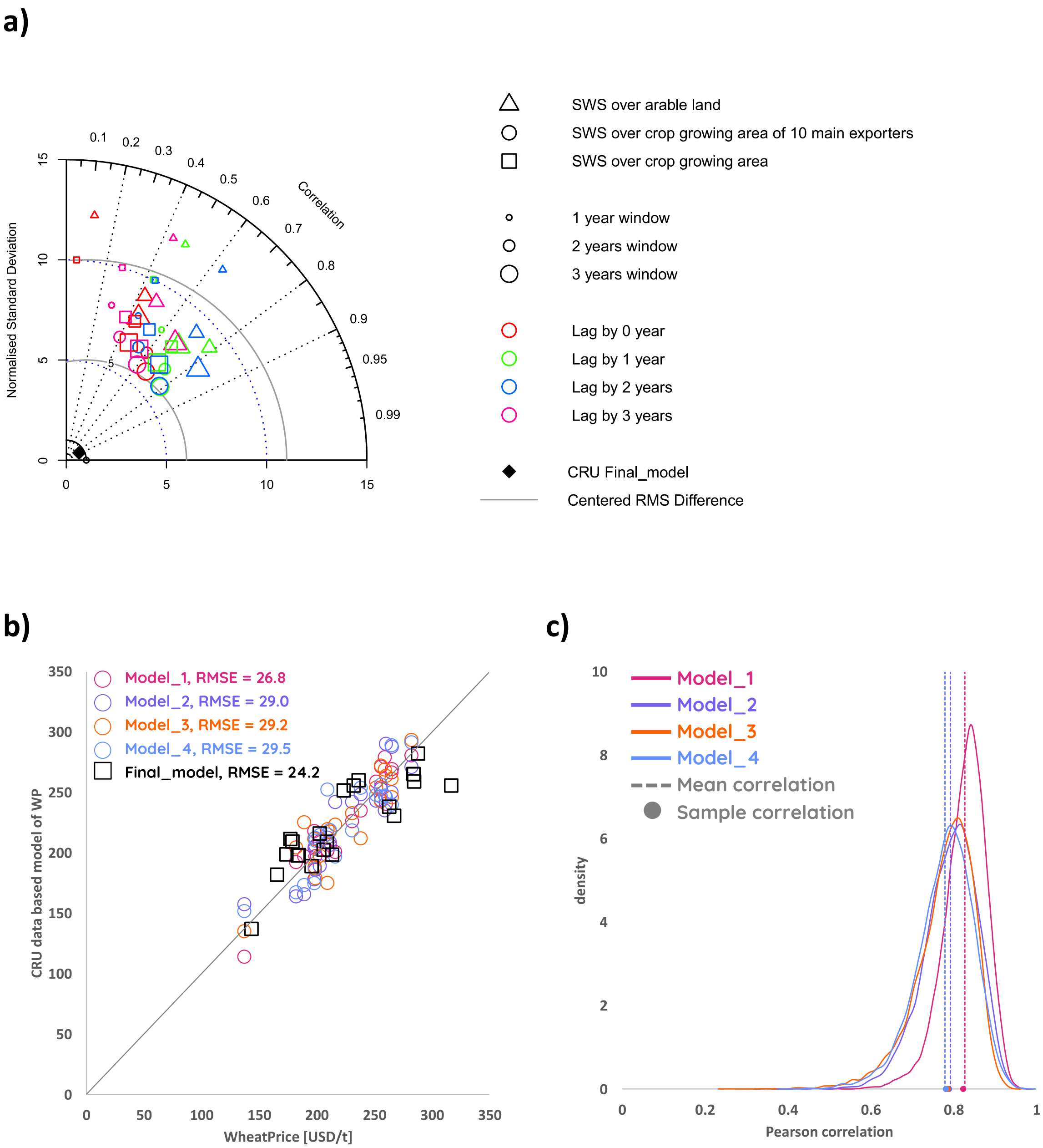

Figure 2. (a) Results of the fit of severe water scarcity (SWS) and the Wheat Price to form crop price models in the form of Taylor diagrams, where different areas, lags (0–3 years) and time windows (1–3 years) of SWS are considered. The diagram visualizes the Pearson correlation coefficient and standard deviation. The black dot indicate the perfect fit (model with a Pearson correlation coefficient $r = 1$ and a root-mean squared error = 0) and the cros the performance of the model ensemble; (b) Comparison of the reported World Bank real wheat price values on the X-axis and its estimates via the ensemble of the 4 linear models and their weighted combination driven by the CRU-derived SWS estimates on the Y-axis; (c) bootstrapping tests of Pearson correlation for the 4 linear models (Table S4 in Supporting Information S1).

(MPI) is based on the No. 3 yellow variety from four shipment locations, including Argentina, Brazil, and the US. The rice price index (RPI) is composed of 9 quotations of different varieties and shipment locations in India, Pakistan, Thailand, Uruguay, and the U.S. These price indices cover the 2000–2023 period, with the index value in January 2000 set to 100 and closely correlate to the pink sheet data of the World Bank and leading to similar results. However, since World Bank provides prices in monetary units, that is USD, this was used as primary source of data. Both the primary International Grains Council (IGC) data and the WPI and FPI annual means are provided in the Data section.

2.4. Climate Data

The simulations of 31 GCMs (Table S3 in Supporting Information S1) from the CMIP6 ensemble and 27 models from the CMIP5 ensemble (Table S4 in Supporting Information S1) were used for predicting SWS (Taylor et al., 2012). These simulations included model runs with specific historical, natural, and anthropogenic forcings from 1861 to 2005 in the case of CMIP5 and 1861 to 2014 in the case of CMIP6 and included 21st century changes in anthropogenic aerosols and greenhouse gases (Vuuren et al., 2011). If a model was associated with multiple simulations, only the first run was used.

All the monthly data needed for the calculations (i.e., mean temperature, sum of precipitation, mean wind speed, mean solar radiation, mean relative humidity and mean sensible and latent heat fluxes) were first spatially interpolated via kriging from the original model grids to a common grid with a 0.5° resolution and then bias-corrected via the delta change method (Feng et al., 2014). The temperature and precipitation data were bias-corrected based on the observed 1961–1990 monthly climatology developed by the Climate Prediction Center (CPC) (Fan & Dool, 2008), whereas the other variables were bias-corrected based on the observed 1961–1990 monthly climatology developed by the CRU of the University of East Anglia (New et al., 1999). This bias correction method ensured that the modeled variables were associated with the same monthly climatology as the CPC or CRU observations during the 1961–1990 period.

In addition to the model simulations, the 0.5° gridded monthly observed temperature, precipitation, and PET data sets developed by the CRU, that is, CRU-TS.4.05 (Harris et al., 2014), were used. These data sets were based on observations collected from thousands of weather stations globally from 1901 to 2024, providing a baseline for validating the CMIP5 and CMIP6 model simulations.

2.5. Standardized Precipitation Evapotranspiration Index (SPEI)

The SPEI (Vicente-Serrano et al., 2010), which is a multiscalar drought index that quantifies drought intensity at various time scales, was adopted. The SPEI was computed based on 1, 3 and 12 months of accumulated surface water deficits and surpluses (i.e., precipitation minus PET). The calculation then employed statistical probability distributions to quantify the drought intensity, termed the 1-, 3-, and 12-month SPEI. The 1-month SPEI is closely related to shallow-layer soil moisture and can be used to evaluate short-term drought variability. The 12-month SPEI is related to the deep-layer soil moisture and long-term drought variability.

The PET was estimated via the FAO-56 Penman–Monteith method for reference grass (Allen et al., 1998) as described by Trnka et al. (2019) using air temperature, relative humidity, wind speed and solar radiation as inputs. In addition to consistent warming (Collins et al., 2013), climate models are consistent in showing regional changes in relative air humidity (Sherwood & Fu, 2014) and vapor pressure deficit. The roles of the wind speed and solar radiation in PET are secondary for future conditions (Fu & Feng, 2014). Owing to the notable impacts of temperature and relative humidity, climate models routinely project increasing PET levels (Scheff & Frierson, 2014).

The values of the 1-, 3-, and 12-month SPEI were calculated based on the monthly precipitation and PET. The snow-melting module developed by Schrier et al. (2007) was also assessed to quantify the impact of snow on the water supply. However, the differences between SWS with and without snow melt were not significant within the growing areas of the three analyzed crops. Therefore, a simplified scheme was implemented that did not account for snow melting. For a given climate model output, the statistical probability distribution parameters (Vicente-Serrano et al., 2010) used to calculate the SPEI were determined based on the modeled monthly data from 1901 to 2000. These parameters were subsequently used to calculate SPEI values in each grid cell from 1860 to 2005 for CMIP5 and 1860–2014 for CMIP6 under the different future emission scenarios. The same procedures were applied to calculate the SPEI from 1901 to 2021 based on the CRU data set.

2.6. Defining Severe Water Scarcity Events and Sensitive Periods

SWS events were first defined to quantify the short- and long-term impacts of water shortages on crops (Table S1 in Supporting Information S1). A grid cell was considered affected by water scarcity only if both the short-term water scarcity indicators (i.e., 1- and 3-month SPEI) and the long-term water scarcity indicators (i.e., 12-month SPEI) reached predefined thresholds (Table S1 in Supporting Information S1). These thresholds were adopted based on prior studies (Blauhut et al., 2015), wherein the probability of drought impact occurrence was estimated

10.1029/2025EF006095

based on the impacts of drought in individual sectors. Since all three considered crops are grown during only part of the year, crop-specific water scarcity sensitivity periods (SPs) were used. These periods were defined as the 4 months prior to the usual crop harvest date and include both the peak vegetative stage (wheat heading and maize and rice flowering) and grain filling for each crop. These 4 months constitute the time of the most intense growth, including the formation of all yield components. For rice, only the first harvest date during a given season was considered.

When the usual harvest date occurred on or later than the 20th day of the month, the SPEI values for the harvest month and the three preceding months were used. When the crop was harvested before the 20th day of the harvest month, the SPEI for the four months prior to the harvest month was used. This offset was used because the crop harvest date, in practice, follows physiological maturity for several days or even weeks (in the case of wheat and maize), and the sensitivity of all three crops to lack of water rapidly decreases at the end of the grain filling stage and after maturity. In fact, drier conditions during harvest are generally beneficial for crop quality and could increase harvest efficiency. In all calculations, calendar months were used.

For each crop-growing grid cell and year, it was first determined whether the cell and year were affected by SWS ($D_i = 1$) or not ($D_i = 0$) during each crop-growing season based on the thresholds defined in Table S1 in Supporting Information S1. For a 1-year window of water scarcity, only events during the harvest year were considered. For a 2-year SWS window, a grid was considered affected by water scarcity ($D_i = 1$) if the SWS thresholds were met either during the harvest year or during the previous harvest year. Similarly, a 3-year window of water scarcity categorized a grid as experiencing SWS if the conditions were met during the SPs of the harvest year or during any of two preceding years. The use of 1-, 2-, and 3-year windows allowed us to examine the impacts of a severe (extreme) water scarcity events affecting multiple regions in sequence, such as the case of wheat production and, to a certain extent, maize production being influenced by the 2010 droughts in Russia and India and the 2012 drought in the USA.

2.7. Relating SWS to Crop Price

In the development of the SWS–crop price model, so-called real prices of all three commodities were used (World Bank, 2025) as well as crop-specific price indices (i.e., WPI, MPI, and RPI). Models were developed using 2000–2021 data with years 1986–1999 and 2022–2024 excluded from the model development. Several SWS based predictors were systematically explored and assessed in hierarchical order. This included the SWS extent in arable land, the given cereal-growing area, and the given cereal-growing area within its 10 largest exporters. The effects of SWS events on prices can vary over time and can materialize with a time lag. To capture this complexity, different time lags were considered, including analyses of (a) the SWS extent window and (b) the cereal price time lag. In any model, the SWS effect on the price accumulated over three windows was considered, that is, the given season (n) and duration window of 1 year (w1), the given season and the preceding season (n; $n-1 = \text{w2}$) and the given season and the two previous seasons (n; $n-1$; $n-2 = \text{w3}$). The cereal price lag accounted for the offset between SWS and price formation. In total, four time lags were cosidered, with lag0 indicating the annual price responding to SWS in the given year, whereas lag$N$ expects the cereal price to lag the SWS extent by N years for N in $\{1,2,3\}$. Roughly, the 3-year lag sets the upper bound to offset any storage capacity for grain reserves. Moreover, both the cereal price index and SWS values and the first-order differences were used. For each crop, $3 \times 3 \times 4 \times 2 = 72$ linear models were formulated (3 SWS grid settings, 3 time windows, 4 time lags and 2 nominal values/first order differences) and evaluated using the Pearson correlation coefficient (r), Theil coefficient and root-mean squared error (RMSE) (Figure 2, Figure S2 and Table S2 in Supporting Information S1). The model performance was captured for all three crops, as shown in Figure 2 and Figure S2 in Supporting Information S1.

In the case of wheat the individual SWS-wheat price models were iteratively combined into the best performing ensemble based on the highest R^2 and lowest RMSE values (Figure S4 in Supporting Information S1). In this case the iterative process resulted in a final ensemble of four models (Figure 2b and Table S2 in Supporting Information S1). These four models, which are based only on SWS, were individually evaluated via the Pearson correlation coefficient by bootstrapping with 10,000 repeats (Figure 2c). This showed that the model performance over the training period was insensitive to any particular season.

The final ensemble of 4 models was optimized by weights to improve R^2. These weights were calculated via the minimum least squares method with positive results, namely, the weights conformed with the defined

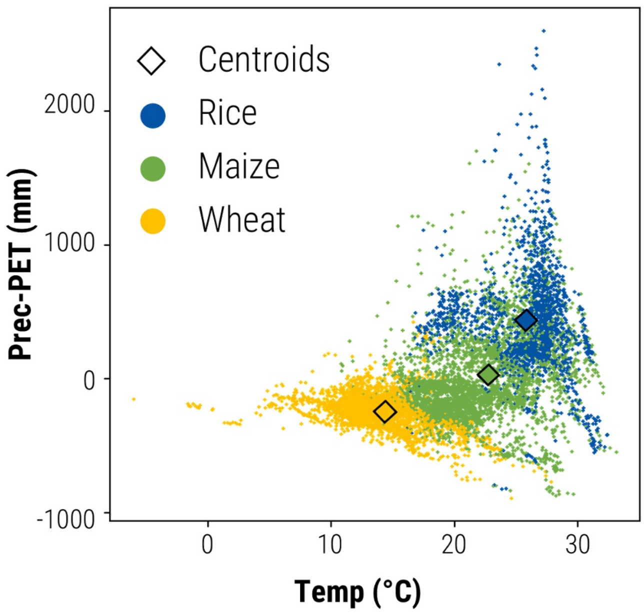

Figure 3. Basic climatological characteristics of the climate model grids growing rice, maize and wheat showing their mean temperatures (X-axis) and the sum of the differences in precipitation and potential evapotranspiration during the 4 months before harvest (Y-axis).

combination of the models given in Table S3 in Supporting Information S1. The final model (Final_model) applies these weights. The weighted values are marked as black rectangles in Figure 2b. Final_model and 4 individual wheat price models from the ensemble were used to estimate the price levels between 1986 and 2024 via the CRU data set (CRU Final_model), resulting in control period benchmark values of the price index, which were compared with those of the WB real wheat price. Figures S5 and S4 in Supporting Information S1 shows estimates of the FPIs from 1986 to 2024 obtained with the model ensemble trained only on the 2000–2021 period.

The grain prices were estimated by Final_model over the control periods of both CMIP6 (31 runs, Table S3 in Supporting Information S1) and CMIP5 (27 runs Table S4 in Supporting Information S1) as annual plus 5 and 10-year means. The CMIP6- and CMIP5-based price estimates are presented as the means and confidence intervals. The uncertainty band is a composite of the 10%/90% uncertainty in the linear regression of Final_model and the 0.05/0.95 quantile of the 31 model outputs based on the CMIP6 GCMs. Figure S6 in Supporting Information S1 shows annual price estimates for each GCM to highlight the internal variability of the price projections.

The relationship between the expected change in the global temperature and the estimated wheat prices was based on the 31 GCM outputs and the changes in the mean annual temperature under all scenarios of all individual global models have been analyzed (Figure 3c). The analysis covered period 1951–2100 and the global wheat price estimates were based on the Final_model.

3. Results

3.1. Sensitivity of Global Rice, Maize and Wheat Prices to SWS

The SWS allows us to express the extent of the area affected by limited water availability during part of the growing season (Trnka et al., 2019), which is specific to a particular crop. It integrates and weighs the severity of water scarcity over global crop-growing areas, capturing cooccurring SWS events. The ability of SWS to explain the variation in the global prices of three major crops (rice, maize and wheat) was evaluated when SWS was aggregated over (a) the total arable land; (b) the growing area for each crop; and (c) the crop-growing areas of the top 10 exporters worldwide (Figure S1 in Supporting Information S1).

The analysis revealed that for rice, no meaningful relationship existed between the SWS-affected area and rice price (Figure S2a in Supporting Information S1). The maize price models explained up to 40% of the global price variability ($p < 0.01$), with the SWS extent in maize-growing regions being the most efficient predictor. These predictions were similarly effective when only the SWS-affected maize growing areas of the top 10 exporters were used (Figure S2b in Supporting Information S1). In case of wheat, the relationship between the SWS-affected area and fluctuations in global prices were much closer (Figure 2a and Table S2 in Supporting Information S1) with four models from the final ensemble explaining between 61% and 68% of wheat price variability.

The different sensitivities of rice, maize and wheat prices to SWS are at least partly explained in Figure 3. Rice is predominantly grown in environments, where rainfall exceeds the PET during the critical part of the growing season (Figure 3), which is defined as 4 months prior to harvest. This is in direct contrast to wheat, which is grown in cooler environments under mostly water-limited conditions. These areas are characterized by climates with PET levels above rainfall. Maize is in this respect grown in "transition zones" between these two situations. The influence of SWS on rice is more often offset by irrigation, which covers 33% of the total harvested area of this rice, and only 15% of that of wheat (Portmann et al., 2010). Also limiting factor in case of rice was existence of multiple harvests which were not fully considered. The overall results indicated that SWS can be used as price predictor in case of wheat and potentially also in case of maize. The Taylor diagrams (Figure 2 and Figure S2 in Supporting Information S1) provided justification for only using wheat in the further analysis, as the rice models performed rather poorly, and the maize models explained less than half of the price variability from SWS variability.

3.2. Estimating the Wheat Price Response to SWS Variation

Four SWS–wheat price models were used to estimate the annual variation in the SWS-affected areas (Figure S3 in Supporting Information S1) on wheat grain prices (Figure 2 and Figure S4 in Supporting Information S1). However, all four models underestimate the impact of high SWS exposure on price variability. The Final_model explained 74% of the interannual wheat price variability from 2000 to 2021, with a relative RMSE of 10.9% for the wheat price (Figure 2a). The relationship between SWS and the global wheat price remained statistically significant ($p < 0.001$) even if the years with peak prices, namely, 2007/2008, 2010/2011, 2018/2019, and 2019/2020, were excluded. Final_model also estimated the wheat prices of 2022, 2023 and 2024 with differences of −16.1%, 17.5% and 35.7%, respectively, which somewhat illustrates the model's capability of predicting beyond the calibration range (Figure 2a, Figure S4 in Supporting Information S1), as these years were not available at the time of model development and estimated the general price levels in the period 1986–1999.

Figure S4 in Supporting Information S1 shows the benchmark test of the Final_model and autoregressive integrated moving average (ARIMA) models as ARIMA approach is frequently used in the commodity price modeling. As expected the ARIMA models captured the price variation only with the time lag (compared with SWS) and performed less satisfactorily (Figure S4 in Supporting Information S1) than the SWS-based ensemble. The additional reason why ARIMA models were not considered further was their limited ability in the price projection captured in Figure S4d in Supporting Information S1.

3.3. Observed and Expected Shifts in SWS Extent and Impact on Wheat Grain Price

Between 1911 and 2020, 5.0% ± 4.2% of the global wheat-growing area was affected by SWS on average, with the maximum extent exceeding 15% in 2000, 2010, 2012, and 2020 (Fig. S3 in Supporting Information S1). The average SWS-affected area exhibited a significant positive trend ($p < 0.001$) between 1911 and 2000, with a 0.5% increase in the number of affected climate grid cells per decade. Between 2011 and 2021, the rate of SWS area increase was even higher, at 2.2%.

The reported WB real wheat prices from 1986 to 2024 occurred within the 5%–95% confidence interval of price estimates of Final_model based on observed CRU data and price estimates of Final_model based on GCM "historical" data (Figure 4). Importantly the prices generated from the GCM control run were ∼13% lower than those estimated by the price models from observed climate data and observed prices (Figure 4a). This finding could be explained by the CMIP6-GCM control run results yielding a lower percentage of the SWS-affected area than that obtained based on the CRU data. Therefore, the mean prices estimated based on the GCM findings were lower than those estimated based on the CRU estimates. However WB real wheat price values were within the 95% confidence intervals (Figures 2d and 3a) of the CRU-based and the CMIP6-GCM control run-based wheat price estimates.

The projected changes in wheat prices based on the CMIP6-based SWS projections are summarized in Figures 4 and 5 as well as Figure S6 in Supporting Information S1. The mean price level is estimated to increase with increasing temperature, but the change till 2050 is likely to be relatively small in comparison with the interannual variation of market wheat prices (Figure 4b and Figure S6b in Supporting Information S1). The mean price level for period 2001–2020 based on estimating SWS from CMIP6 data for this period was estimated at 193 ± 22 USD/t; for both SSP1-2.6 and SSP5-8.5. Mean price level for the period 2031–2050 was estimated to be 294 ± 18 UDS/t (SSP1-2.6) and 327 ± 33 USD/t (SSP5-8.5) as Figure 4 shows. There were no significant ($p = 0.01$) differences among the price estimates obtained by the individual SSPs from 2011 to 2040, but the price estimates among the SSPs sharply diverged in the late 21st century (Figure S6 in Supporting Information S1) and for more intense warming (Figure 5). The likelihood of widespread SWS events increased in some GCMs, and the upper price estimates accordingly shifted. The modeled prices exhibited slower growth up to +1°C of warming, with a higher rate of increase between 1 and 2°C, followed by a slightly lower rate of price growth under more intense warming (Figure 5). The increase in global mean temperatures by 2°C was estimated to lead to grain prices around 273 USD/t (Figure S6 in Supporting Information S1) while increase by 3°C results in mean price estimate of 364 USD/t. Difference between using CMIP6 and CMIP5 GCMs ensembles is relatively small (Figure S7 in Supporting Information S1).

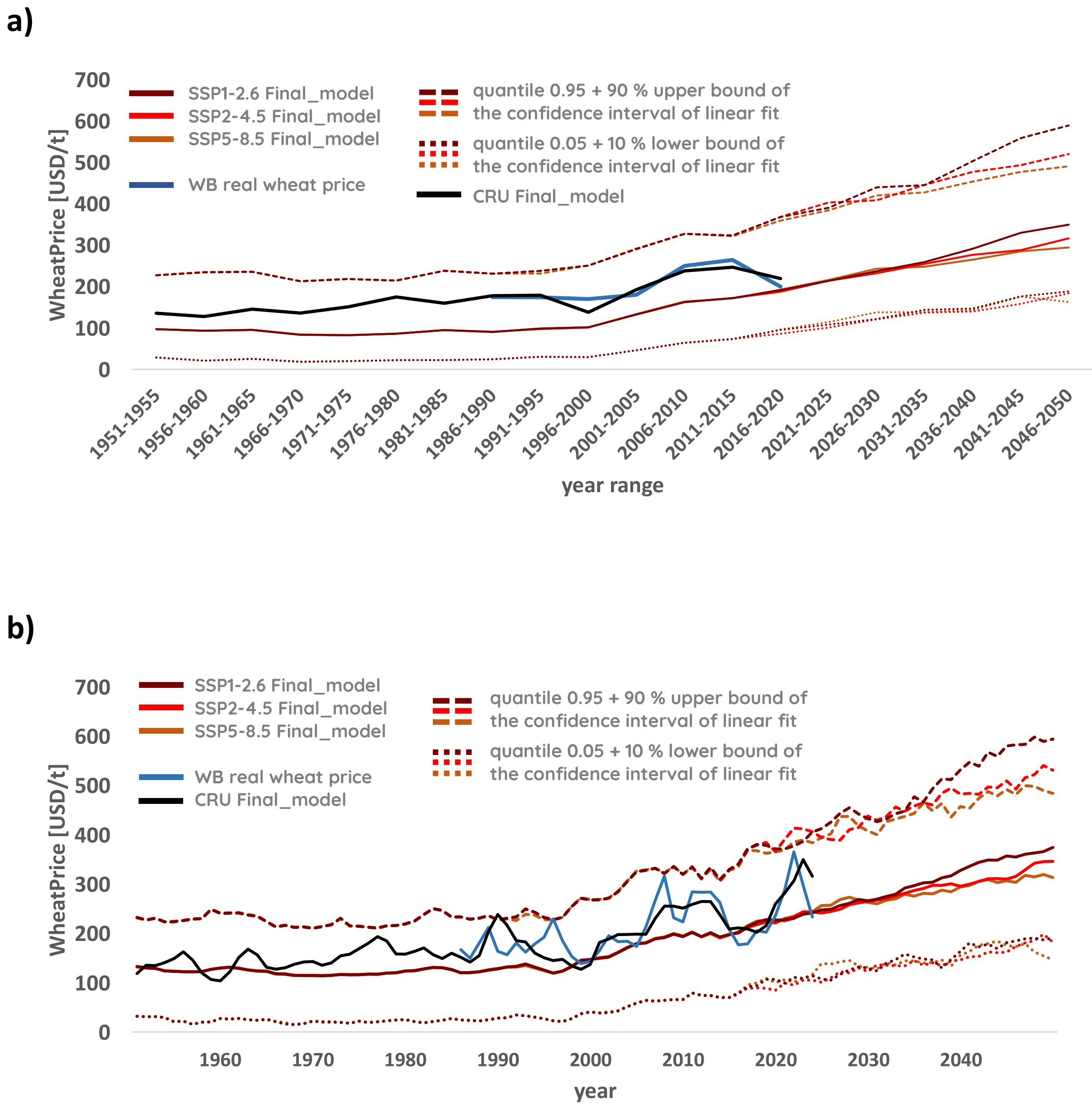

Figure 4. (a) Time series of the reported (blue) and estimated wheat price values via the Final_mocel for the 2000–2024 period using as climate inputs both observed Climate Research Unit data (black) and for CMIP6 global climate model model ensemble (red tones) median (solid line) and 5th and 95th quantile. The price values are expressed as 5-year averages; (b) The same as (a) but for annual values (for more details see also Figure S5 in Supporting Information S1).

4. Discussion

4.1. Context of the Study Estimates

Despite its importance, the studies focusing on impact of changes in climate variability on agricultural prices remain limited (Myers et al., 2022). Traditionally, the literature on agricultural production, consumption and market impacts has concentrated on the analysis of global mean temperature changes due to climate change by implementing 30-year moving averages of crop model outputs in partial and general equilibrium economic models (Nelson et al., 2014; Van Meijl et al., 2018). Figure S8 in Supporting Information S1 shows the effects of climate change on agricultural prices obtained via conventional economic analysis. The Global Economic Model Intercomparison Activity of the Agricultural Model Intercomparison and Improvement Project (AgMIP) produced a range of price projections by midcentury based on numerous combinations of climatic and socioeconomic

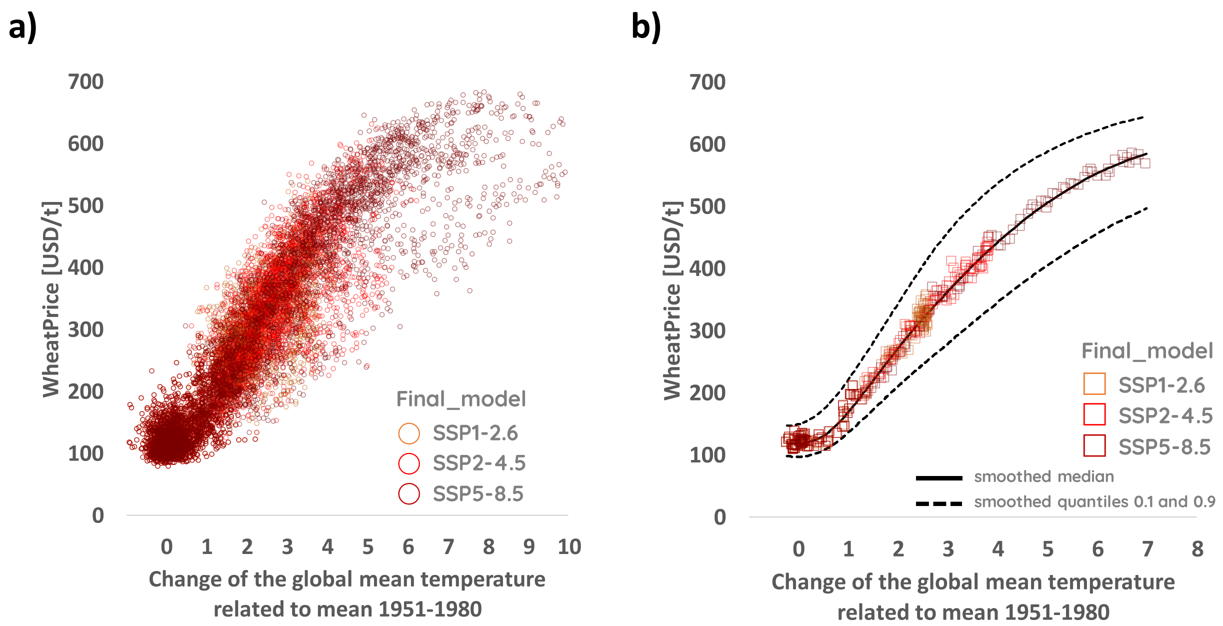

Figure 5. Summary of the expected wheat price in USD/t related to the change in the global mean temperature with baseline 1951–1980 estimated using 31 CMIP6 global climate models (GCMs) with (a) capturing the Scatter of individual data points representing combinations of years (1951–2100), shared socioeconomic pathways (SSPs) and individual GCMs; (b) Annual medians for each SSP over all GCMs are displayed as square markers. A smoothed line fitted across all 450 medians (3 SSPs * 150 years) represents the overall trend, with dashed lines indicating the corresponding quantiles 0.1 and 0.9.

factors. The ensemble of participating models (9 models: 5 computable general equilibrium (CGE) models and 4 partial equilibrium (PE) models) projected a 3%–32% wheat price increase by 2050 under SSP2 and RCP8.5, with no significant difference between the CGE and PE models relative to the baseline scenario (Nelson et al., 2014). The most recent study (Nelson et al., 2014) projected an increase in cereal prices of 1%–29% across different SSPs and 3°C warming using an ensemble of eight economic models (5 PE models, 2 CGE models and 1 integrated assessment model). These studies have paid little or no attention to the analysis of extremes in relevant regions either from the viewpoint of major exporting or importing regions. On the other hand, the effects of extreme events, such as drought and heat, on grain prices have been studied at the country and regional levels (Schaub & Finger, 2020), including investigations of the effects of increasing grain prices on conflict and political stability in low-income countries (Sternberg, 2012) via econometrics. Furthermore, the supply response of the Global North and South to past weather shocks has also been explored as a mechanism for buffering out the effects of climate variability on the global food supply and prices (Chung et al., 2014; Lybbert et al., 2014); this has led to a gap between the increased understanding of the influence of long-term climate change on agricultural production and the economy as a whole and a lack of knowledge regarding the short-term impacts of SWS events (Frieler et al., 2017).

The results of our study indicate that projected increase in the SWS extent and frequency may result (if other parameters are kept the same) to quite high increase of the wheat prices. A review by Green et al. (2013) indicates that the effects of cereal price increases on food consumption in 162 countries revealed that a 1% increase in cereal prices (a deviation from its long-term trend) could lower food consumption by approximately 0.61%. Thus, according to the projections here, food consumption could be forced to decrease by 27%–38% by 2050 due to SWS. In general, households that spend more than 50% of their income on food are at medium risk of food insecurity from increases in the price of wheat (Smith & Subandoro, 2007). In low-income countries, households typically spend close to 60% of their income on food (e.g., 56% in Nigeria), with more than a third going toward staples such as vegetables and cereals (World Bank Group, 2019). Low-income households cannot switch to less expensive foods and will be forced to increase spending on basic staples, lower the quality of their diets, or even limit the amount of the most inexpensive foods consumed while also reducing nonfood expenditures (Lele et al., 2016). The negative impacts are even worse among poor urban households, which are typically net buyers of food, whereas households that are net sellers of agricultural and food products would increase their income (World Bank Group, 2019) unless the yields are reduced by SWS events. Considering the ongoing trend of urbanization, with 68% of the global population projected to live in cities by 2050 (UN-Habitat, 2022), the pool of households that will be negatively affected by increased wheat prices will continue to increase (Dadi et al., 2022; Janvry & Sadoulet, 2011).

The projected increase in food price impacts of SWS events thus require urgent attention in terms of adaptation measures on the one hand and disaster-relief systems on the other hand. On the adaptation side, adjusting sowing dates (Fodor et al., 2017), changing crops and/or growing regions (Mourtzinis et al., 2019), upgrading and expanding storage facilities (Hertel et al., 2023; Marchand et al., 2016), and facilitating intra- and international trade activities appear to be potential strategies. Trade was demonstrated to help reduce the number of people at risk of hunger resulting from slow-onset climate change (Janssens et al., 2020), although increased specialization could lead to a concentration in production locations, yielding more volatile world markets (e.g., price spikes due to SWS events).

Clearly, the SWS extent (Trnka et al., 2019) is a significant but not unique factor affecting crop product prices. Pests and diseases, such as fungal diseases (Godfray et al., 2016) or locust outbreaks (Peng et al., 2020), economic factors, such as demand shocks, volatile oil prices and exchange rates (Tadasse et al., 2016), grain storage capacity (Schewe et al., 2017), political and military conflicts or policy responses (Headey, 2011) play a role and may coincide with drought events. The Ukraine–Russia conflict illustrates the response of the market and its instability, as both countries are major exporters of wheat grain and other agricultural commodities such as oilseed, which is integral to many cereal-based crop rotations. The war in Ukraine has significantly impacted the price of food products (Glauber & Laborde Debucquet, 2023), leading to increasing exports from other countries to partially compensate for the lack of supply from Ukraine and Russia (Chepelliev et al., 2022) and was one of the reasons why years 2022–2024 were not included in the model development data set. Compared with March 2021, the prices of wheat and maize rose by 58% and 38%, respectively, (IGC, 2022) in 2022. This price increase has the same order of magnitude of influence as changes that could partially be attributed to SWS events over the past two decades (Figures 4a and 4b). Obviously, the intensity and duration of military conflicts are inherently difficult to predict. In contrast, the increased occurrence of SWS events under future climate conditions is less uncertain (Figure 4 and Figure S3 in Supporting Information S1), and the proposed Final_model may represent a realistic estimate of future annual price levels.

As described in the data section, the study uses the mean annual commodity prices expressed as the annual mean and it is not possible to account for the regional price differences or price variations on a scale shorter than 1 year, which can be significant. However, the aim of this study is to analyze whether changes in the extent of overall global water scarcity can affect global commodity prices and, if so, to estimate their likely mean level as well as interannual variation. As shown above the SWS concept shows to be robust in this respects and thus provides meaningful projections compared to the simple ARIMA models (Figures S3c and S3d in Supporting Information S1).

4.2. Study Assumptions

The estimates of crop price response to SWS builds on a number of assumptions, which were invoked to ensure that the SWS extent is primarily a function of changing climate conditions. It was assumed that the current wheat-growing areas, their relative weights and the top 10 exporting countries would remain unchanged during the time frame of the analysis. Thus, the potential benefit of shifting wheat production to other agricultural land with a lower SWS probability could lower the model reliability. However, two findings suggest that the conclusions drawn here are little sensitive to this simplification. First, two out of the four models in the final model ensemble are based on SWS occurrence across the entire arable land area; thus, a change in the wheat-growing area would generate no effect. Second, the data revealed that there is little to be gained globally in terms of decreasing SWS exposure by shifting wheat-producing areas both within and outside the present wheat-growing areas, as SWS exposure increases at a similar pace across all regions as already shown by Trnka et al. (2019).

Numerous studies have argued that some or all of the negative impacts of global warming on wheat yields might be ameliorated by increasing atmospheric CO_2 concentrations combined with adaptation strategies (Challinor et al., 2014; Lobell, 2014). Although water use is reduced under elevated CO_2 levels (Manderscheid & Weigel, 2007) and may alleviate moderate dry spells, recent studies have also reported that drought stress, when combined with severe heat, cannot be compensated for by elevated CO_2 concentrations (Jin et al., 2018; Schauberger et al., 2017). These findings are not surprising. While the water use efficiency is proportional to the atmospheric CO_2 concentration, it is inversely proportional to the vapor pressure deficit, which is projected to increase exponentially with increasing air temperature. Additionally, some models (Dai et al., 2018) compared future drying in model simulations with and without considering plant physiology in response to increasing CO_2 levels. They reported that the plant physiological response to increasing CO_2 concentrations was secondary, suggesting that the impact of CO_2 fertilization on future drought severity is limited. It was therefore assumed that the effects of SWS estimated here cannot be alleviated by increased CO_2 levels and that SWS represents a reliable indicator of potential water stress irrespective of CO_2 levels.

It is also likely that increased temperatures accelerate crop development, leading to earlier maturity, which might lead to the avoidance of SWS events for wheat crops by shifting and/or shortening the crop-growing season. Therefore, the effect of shifting the harvest earlier in the year was evaluated. A significant reduction in the extent of the SWS-affected area was found, when looking at a shorter growing season. However the advancement in the harvest date was insufficient in terms of reducing the SWS-affected areas to the levels from 1951 to 1990, as already shown elsewhere (Trnka et al., 2019). In addition, significant shifts in the cropping calendar affect not only wheat crops but entire crop rotations, and there is high uncertainty in how these shifts will eventually occur in many regions worldwide and what their effects on productivity will be (Lobell, 2014).

The empirical makeup of the model assumes that the exporting countries in the future will not change relative to the present situation (Figure 1 and Figure S1 in Supporting Information S1). In the case of wheat, North America, the European Union, and Russia represent approximately 70% of global exports (Figure S9 in Supporting Information S1). Notably, cereal yields are characterized by large differences between high- and low-income countries (FAO, 2017). In 2018, the average grain yield in high-income countries was fourfold greater than that in low-income countries. Closing yield gaps across wheat-growing areas could be an efficient way to increase resilience to SWS-driven price increases. However, major shifts in the patterns of exporting countries will require substantial infrastructure investments (storage, transport, port facilities, etc.) to allow these countries meaningful access to global markets. Interestingly, the increase in the SWS-affected area under future scenarios is so widespread that increasing the resilience of wheat to SWS by rearranging production among the top producing areas would generate only limited benefits or would have to occur at the expense of other crops, that is, maize and rice. Here, we assumed that the final use and consumption of these crops would basically not change. Dietary change toward more animal products in low-income countries or more sustainable diets in the most developed countries was not considered and as Rulli et al. (2024) pointed out the "sustainable" diets may have significant impact on World's agriculture. However, since wheat is one of the basic foods for humans, this may not greatly change the consumption of wheat grains. The Final_model also did not account for the change in global population nor breeding improvement. However as Guarin et al. (2022) study suggests the improved canopy photosynthesis can lead up to ~37% increase in the mean global annual wheat production without expanding cropping area. This increase would be enough to meet the lower estimate of the projected grain demand in 2050 driven by population increase.

It was further assumed that the extent and influence of irrigation did not significantly change. Importantly, the global extent of irrigated croplands increased approximately fivefold during the 20th century, and the current global irrigated area continually increases (Siebert et al., 2015). The three largest crop irrigators globally are China (53.8 Mha), India (57.3 Mha), and the USA (27.9 Mha) (Thenkabail et al., 2009), with rice and maize as the primary irrigated crops. However, these countries are among the regions that are projected to suffer increasing freshwater limitations under most climate change scenarios. Recent analyses have estimated that a reversion of 20–60 Mha of cropland from irrigated to rainfed management or from full to supplementary irrigation is needed by the end of the century in these three countries to balance the irrigation water supply and demand. While there is potential to increase the irrigated area of wheat and thus reduce SWS impacts, this increase must be accompanied by reductions in other current crops (e.g., rice, maize, and cotton) and/or increases in irrigation efficiency. Additionally, the alleviating effect of irrigation on SWS event impacts is likely to be limited, as any SWS event intrinsically includes at least a 12-month drought period before harvest. It may be assumed that during SWS events, the availability of water resources for irrigation in many regions is more limited than that in normal years.

Directly accounting for changes in energy prices is considered the second most important factor affecting the cost of cereal production (Conceição & Mendoza, 2009; Enghiad et al., 2017) after climate was not explicitly considered here. Energy prices play a fundamental role in the cost of agricultural inputs, as energy and fertilizer prices are highly correlated (Kalkuhl et al., 2016). However, both the globally increasing demand for energy and the efforts to curb the use of fossil fuels are likely to increase energy prices, not decrease them, at least in the short term. With ongoing political conflicts and sanctions on major oil- and gas-producing countries, volatility in energy and crop prices is unlikely to decrease in the short term (Wang et al., 2022).

The derived relationship between SWS events and price hikes in wheat encompasses multiple causal factors that may not be solely related to actual yield reductions. Since yield reporting is more prone to reporting distortions than market prices are, the yield analysis has been bypassed here in favor of a direct relationship between SWS and price indicators such as WPI and FPI, which are less prone to reporting distortions. However, market prices are undoubtedly influenced by speculations and uncertainties in the response of cereal-producing countries during SWS events even when yield reductions are minor.

5. Conclusions

Regardless of the discussed assumptions, the SWS–wheat price relations could be in our view considered robust and warrant their inclusion in the projected impacts of the SWS-affected area on wheat prices. In light of the crop price volatility over past 20 years, the projected increase in space–time coherent SWS occurrence cannot be overlooked in any estimates of future price levels, at least in the case of wheat and to some extent maize. The sensitivity of wheat prices to SWS occurrence stems from the fact that out of the three main cereal crops, wheat is grown mostly under the least favorable soil moisture conditions (Figure 3). It therefore cannot be readily replaced by crop of similar nutritional qualities even more tolerant to drought, as principally there is no such crop. The sensitivity of what prices to SWS reported by this study should be subjected even more in-depth systematic research because wheat represents globally the most important crop in terms of area, calorie supply and volume of international trade (Figure 1).

Conflict of Interest

The authors declare no conflicts of interest relevant to this study.

Availability Statement

The list of top 10 exporters is based on (https://www.fao.org/faostat/en/#data/TCL). The values of Prec-PET and Temperature for wheat, rice and maize growing grids were calculated based on the CRU data (https://data.ceda.ac.uk/badc/cru/data/cru_ts) and are part of the data repository. Severe water scarcity (SWS) estimates were based on SPEI calculations using CRU data (https://data.ceda.ac.uk/badc/cru/data/cru_ts) and for the climate models presented in the data repository. The future climate data have been based on publicly available CMIP6 and CMIP5 (ESGF nodes: https://esgf-metagrid.cloud.dkrz.de/search) and the estimated SWS are included in the data repository. The wheat price index data were provided by International Grain Council (https://www.igc.int/en/markets/marketinfo-goi.aspx) and Farm index data are provided by USDA (https://fred.stlouisfed.org/series/WPU0121). The data files used for Figures 1–3 as well as Figures S1–S8 in Supporting Information S1 are provided separate folders in the data repository (Trnka et al., 2025) in standard formats (cvs or geo-tiffs).

Acknowledgments

The authors thank Anastassios Haniotis for the valuable comments and suggestions. This study was supported by AdAgriF–Advanced methods of greenhouse gas emission reduction and sequestration in agriculture and forest landscapes for climate change mitigation (CZ.02.01.01/00/22_008/0004635). Rothamsted Research received Grant-aided support from the Biotechnology and Biological Sciences Research Council (BBSRC) through the Delivering Sustainable Wheat strategic Program (BB/X011003/1).

References

Allen, R. G., Pereira, L. S., Raes, D., & Smith, M. (1998). Crop evapotranspiration–Guidelines for computing crop water requirements. In *FAO irrigation and drainage paper 56*. https://doi.org/10.1016/j.eja.2010.12.001

Anderson, W., Baethgen, W., Capitanio, F., Ciais, P., Cook, B. I., Cunha, C. G., et al. (2023). Climate variability and simultaneous breadbasket yield shocks as observed in long-term yield records. *Agricultural and Forest Meteorology*, *331*, 109321. https://doi.org/10.1016/j.agrformet.2023.109321

Baker, J. S., Havlík, P., Beach, R., Leclère, D., Schmid, E., Valin, H., et al. (2018). Evaluating the effects of climate change on US agricultural systems: Sensitivity to regional impact and trade expansion scenarios. *Environmental Research Letters*, *13*(6), 064019. https://doi.org/10.1088/1748-9326/AAC1C2

Blauhut, V., Gudmundsson, L., & Stahl, K. (2015). Towards Pan-European drought risk maps: Quantifying the link between drought indices and reported drought impacts. *Environmental Research Letters*, *10*(1), 014008. https://doi.org/10.1088/1748-9326/10/1/014008

Challinor, A. J., Watson, J., Lobell, D. B., Howden, S. M., Smith, D. R., & Chhetri, N. (2014). A meta-analysis of crop yield under climate change and adaptation. *Nature Climate Change 2014*, *4*(4), 287–291. https://doi.org/10.1038/nclimate2153

Chepelliev, M., Maliszewska, M., & Pereira, M. S. E. (2022). Effects on trade and income of developing countries. In M. Ruta (Ed.), *The impact of the war in Ukraine on global trade and investment* (pp. 11–26). World Bank Group.

Chung, U., Gbegbelegbe, S., Shiferaw, B., Robertson, R., Yun, J. I., Tesfaye, K., et al. (2014). Modeling the effect of a heat wave on maize production in the USA and its implications on food security in the developing world. *Weather and Climate Extremes*, *5–6*(1), 67–77. https://doi.org/10.1016/J.WACE.2014.07.002

Collins, M., Knutti, R., Arblaster, J., Dufresne, J.-L., Fichefet, T., Friedlingstein, P., et al. (2013). Long-term climate change: Projections, commitments and irreversibility. In T. F. Stocker, D. Qin, G.-K. Plattner, M. Tignor, S. K. Allen, J. Boschung, et al. (Eds.), *Climate change 2013: The physical science basis. Contribution of working group I to the fifth assessment report of the intergovernmental panel on climate change* (pp. 1029–1136). Cambridge University Press. Retrieved from http://www.climatechange2013.org/images/report/WG1AR5_Chapter12_FINAL.pdf

Conceição, P., & Mendoza, R. U. (2009). Anatomy of the global food crisis. *Third World Quarterly*, *30*(6), 1159–1182. https://doi.org/10.1080/01436590903037473

Dadi, W., Mulegeta, M., & Simie, N. (2022). Urbanization and its effects on income diversification of farming households in Adama district, Ethiopia. *Cogent Economics and Finance*, *10*(1), 2149447. https://doi.org/10.1080/23322039.2022.2149447

Dai, A., Zhao, T., & Chen, J. (2018). Climate change and drought: A precipitation and evaporation perspective. *Current Climate Change Reports 2018*, *4*(3), 301–312. https://doi.org/10.1007/S40641-018-0101-6

de Janvry, A., & Sadoulet, E. (2011). Subsistence farming as a safety net for food-price shocks. *Development in Practice*, *21*(4–5), 472–480. https://doi.org/10.1080/09614524.2011.561292

Enghiad, A., Ufer, D., Countryman, A. M., & Thilmany, D. D. (2017). An overview of global wheat market fundamentals in an era of climate concerns. *International Journal of Agronomy*, *2017*, 1–15. https://doi.org/10.1155/2017/3931897

Fan, Y., & van den Dool, H. (2008). A global monthly land surface air temperature analysis for 1948–present. *Journal of Geophysical Research*, *113*(D1), 1103. https://doi.org/10.1029/2007JD008470

FAO. (2017). The future of food and agriculture - Trends and challenges.

FAO. (2022). Faostat. Retrieved from https://www.fao.org/faostat/en

Feng, S., Hu, Q., Huang, W., Ho, C. H., Li, R., & Tang, Z. (2014). Projected climate regime shift under future global warming from multi-model, multi-scenario CMIP5 simulations. *Global and Planetary Change*, *112*, 41–52. https://doi.org/10.1016/J.GLOPLACHA.2013.11.002

Fodor, N., Challinor, A., Droutsas, I., Ramirez-Villegas, J., Zabel, F., Koehler, A. K., & Foyer, C. H. (2017). Integrating plant science and crop modeling: Assessment of the impact of climate change on soybean and maize production. *Plant and Cell Physiology*, *58*(11), 1833–1847. https://doi.org/10.1093/PCP/PCX141

Frieler, K., Schauberger, B., Arneth, A., Balkovič, J., Chryssanthacopoulos, J., Deryng, D., et al. (2017). Understanding the weather signal in national crop-yield variability. *Earth's Future*, *5*(6), 605–616. https://doi.org/10.1002/2016EF000525

Fu, Q., & Feng, S. (2014). Responses of terrestrial aridity to global warming. *Journal of Geophysical Research: Atmospheres*, *119*(13), 7863–7875. https://doi.org/10.1002/2014JD021608

Glauber, J. W., & Laborde Debucquet, D. (2023). How will Russia's invasion of Ukraine affect global food security? In J. W. Glauber & D. Laborde Debucquet (Eds.), *The Russia-Ukraine conflict and global food security* (p. 196). International Food Policy Research Institute. https://doi.org/10.2499/9780896294394

Godfray, H. C. J., Mason-D'croz, D., & Robinson, S. (2016). Food system consequences of a fungal disease epidemic in a major crop. *Philosophical Transactions of the Royal Society B: Biological Sciences*, *371*(1709), 20150467. https://doi.org/10.1098/RSTB.2015.0467

Green, R., Cornelsen, L., Dangour, A. D., Honorary, R. T., Shankar, B., Mazzocchi, M., & Smith, R. D. (2013). The effect of rising food prices on food consumption: Systematic review with meta-regression. *BMJ*, *346*(7915), f3703. https://doi.org/10.1136/BMJ.F3703

Guarin, J. R., Martre, P., Ewert, F., Webber, H., Dueri, S., Calderini, D., et al. (2022). Evidence for increasing global wheat yield potential. *Environmental Research Letters*, *17*(12), 124045. https://doi.org/10.1088/1748-9326/aca77c

Harris, I., Jones, P. D., Osborn, T. J., & Lister, D. H. (2014). Updated high-resolution grids of monthly climatic observations – The CRU TS3.10 dataset. *International Journal of Climatology*, *34*(3), 623–642. https://doi.org/10.1002/JOC.3711

Hasegawa, T., Fujimori, S., Havlík, P., Valin, H., Bodirsky, B. L., Doelman, J. C., et al. (2018). Risk of increased food insecurity under stringent global climate change mitigation policy. *Nature Climate Change 2018*, *8*(8), 699–703. https://doi.org/10.1038/s41558-018-0230-x

Hasegawa, T., Wakatsuki, H., Ju, H., Vyas, S., Nelson, G. C., Farrell, A., et al. (2022). A global dataset for the projected impacts of climate change on four major crops. *Scientific Data 2022*, *9*(1), 1–11. https://doi.org/10.1038/s41597-022-01150-7

Headey, D. (2011). Rethinking the global food crisis: The role of trade shocks. *Food Policy*, *36*(2), 136–146. https://doi.org/10.1016/J.FOODPOL.2010.10.003

Heinicke, S., Frieler, K., Jägermeyr, J., & Mengel, M. (2022). Global gridded crop models underestimate yield responses to droughts and heatwaves. *Environmental Research Letters*, *17*(4), 044026. https://doi.org/10.1088/1748-9326/AC592E

Hertel, T., Elouafi, I., Tanticharoen, M., & Ewert, F. (2023). Diversification for enhanced food systems resilience. In J. von Braum, K. Afsana, L. O. Fresco, & M. H. A. Hassan (Eds.), *Science and innovations for food systems transformation* (pp. 207–2016). Springer. https://doi.org/10.1007/978-3-031-15703-5

Hoekstra, A. Y., Mekonnen, M. M., Chapagain, A. K., Mathews, R. E., & Richter, B. D. (2012). Global monthly water scarcity: Blue water footprints versus blue water availability. *PLoS One*, *7*(2), e32688. https://doi.org/10.1371/JOURNAL.PONE.0032688

IGC. (2022). IGC grains and oilseeds index. Retrieved from https://www.igc.int/en/markets/marketinfo-goi.aspx

Janssens, C., Havlík, P., Krisztin, T., Baker, J., Frank, S., Hasegawa, T., et al. (2020). Global hunger and climate change adaptation through international trade. *Nature Climate Change 2020*, *10*(9), 829–835. https://doi.org/10.1038/s41558-020-0847-4

Jin, Z., Ainsworth, E. A., Leakey, A. D. B., & Lobell, D. B. (2018). Increasing drought and diminishing benefits of elevated carbon dioxide for soybean yields across the US Midwest. *Global Change Biology*, *24*(2), e522–e533. https://doi.org/10.1111/GCB.13946

Kalkuhl, M., von Braun, J., & Torero, M. (2016). Food price volatility and its implications for food security and policy. *Food Price Volatility and Its Implications for Food Security and Policy*, 1–626. https://doi.org/10.1007/978-3-319-28201-5/COVER

Lele, U., Masters, W. A., Kinabo, J., Meenakshi, J. V., Ramaswami, B., Tagwireyi, J., & Goswami, S. (2016). Measuring food and nutrition security: An independent technical assessment and user's guide for existing indicators. *Food Security Information Network, Measuring Food and Nutrition Security Technical Working Group*.

Lobell, D. B. (2014). Climate change adaptation in crop production: Beware of illusions. *Global Food Security*, *3*(2), 72–76. https://doi.org/10.1016/J.GFS.2014.05.002

Lybbert, T. J., Smith, A., & Sumner, D. A. (2014). Weather shocks and inter-hemispheric supply responses: Implications for climate change effects on global food markets. *Climate Change Economics*, *5*(4), 1450010. https://doi.org/10.1142/s2010007814500109

Manderscheid, R., & Weigel, H. J. (2007). Drought stress effects on wheat are mitigated by atmospheric CO2 enrichment. *Agronomy for Sustainable Development 2007*, *27*(2), 79–87. https://doi.org/10.1051/AGRO:2006035

Marchand, P., Carr, J. A., Dell'Angelo, J., Fader, M., Gephart, J. A., Kummu, M., et al. (2016). Reserves and trade jointly determine exposure to food supply shocks. *Environmental Research Letters*, *11*(9), 095009. https://doi.org/10.1088/1748-9326/11/9/095009

Mehrabi, Z., & Ramankutty, N. (2019). Synchronized failure of global crop production. *Nature Ecology & Evolution*, *3*(5), 780–786. https://doi.org/10.1038/s41559-019-0862-x

Mekonnen, M. M., & Hoekstra, A. Y. (2011). The green, blue and grey water footprint of crops and derived crop products. *Hydrology and Earth System Sciences*, *15*(5), 1577–1600. https://doi.org/10.5194/HESS-15-1577-2011

Mourtzinis, S., Specht, J. E., & Conley, S. P. (2019). Defining optimal soybean sowing dates across the US. *Scientific Reports 2019*, *9*(1), 1–7. https://doi.org/10.1038/s41598-019-38971-3

Myers, S., Fanzo, J., Wiebe, K., Huybers, P., & Smith, M. (2022). Current guidance underestimates risk of global environmental change to food security. *BMJ*, *378*, e071533. https://doi.org/10.1136/BMJ-2022-071533

Nelson, G. C., Valin, H., Sands, R. D., Havlík, P., Ahammad, H., Deryng, D., et al. (2014). Climate change effects on agriculture: Economic responses to biophysical shocks. *Proceedings of the National Academy of Sciences of the United States of America*, *111*(9), 3274–3279. https://doi.org/10.1073/pnas.1222465110

Nendel, C., Reckling, M., Debaeke, P., Schulz, S., Berg-Mohnicke, M., Constantin, J., et al. (2023). Future area expansion outweighs increasing drought risk for soybean in Europe. *Global Change Biology*, *29*(5), 1340–1358. https://doi.org/10.1111/GCB.16562

New, M., Hulme, M., & Jones, P. (1999). Representing twentieth-century space–time climate variability. Part I: Development of a 1961–90 mean monthly terrestrial climatology. *Journal of Climate*, *12*(3), 829–856. https://doi.org/10.1175/1520-0442(1999)012<0829:RTCSTC>2.0.CO;2

OECD, & FAO. (2020). OECD-FAO agricultural outlook 2020-2029. https://doi.org/10.1787/1112c23b-en

Peng, W., Ma, N. L., Zhang, D., Zhou, Q., Yue, X., Khoo, S. C., et al. (2020). A review of historical and recent locust outbreaks: Links to global warming, food security and mitigation strategies. *Environmental Research*, *191*, 110046. https://doi.org/10.1016/J.ENVRES.2020.110046

Portmann, F. T., Siebert, S., & Döll, P. (2010). MIRCA2000-Global monthly irrigated and rainfed crop areas around the year 2000: A new high-resolution data set for agricultural and hydrological modeling. *Global Biogeochemical Cycles*, *24*(1). https://doi.org/10.1029/2008gb003435

Ramankutty, N., Evan, A. T., Monfreda, C., & Foley, J. A. (2008). Farming the planet: 1. Geographic distribution of global agricultural lands in the year 2000. *Global Biogeochemical Cycles*, *22*(1), 1003. https://doi.org/10.1029/2007GB002952

Rulli, M. C., Sardo, M., Ricciardi, L., Govoni, C., Galli, N., Chiarelli, D. D., et al. (2024). Meeting the EAT-lancet healthy diet target while protecting land and water resources. *Nature Sustainability*, *7*(12), 1651–1661. https://doi.org/10.1038/s41893-024-01457-w

Schaub, S., & Finger, R. (2020). Effects of drought on hay and feed grain prices. *Environmental Research Letters*, *15*(3), 34014. https://doi.org/10.1088/1748-9326/ab68ab

Schauberger, B., Archontoulis, S., Arneth, A., Balkovic, J., Ciais, P., Deryng, D., et al. (2017). Consistent negative response of US crops to high temperatures in observations and crop models. *Nature Communications 2017*, *8*(1), 1–9. https://doi.org/10.1038/ncomms13931

Scheff, J., & Frierson, D. M. W. (2014). Scaling potential evapotranspiration with greenhouse warming. *Journal of Climate*, *27*(4), 1539–1558. https://doi.org/10.1175/JCLI-D-13-00233.1

Schewe, J., Otto, C., & Frieler, K. (2017). The role of storage dynamics in annual wheat prices. *Environmental Research Letters*, *12*(5), 054005. https://doi.org/10.1088/1748-9326/AA678E

Sherwood, S., & Fu, Q. (2014). A drier future? *Science*, *343*(6172), 737–739. https://doi.org/10.1126/SCIENCE.1247620/SUPPL_FILE/SHERWOOD.SM.PDF

Siebert, S., Kummu, M., Porkka, M., Döll, P., Ramankutty, N., & Scanlon, B. R. (2015). A global data set of the extent of irrigated land from 1900 to 2005. *Hydrology and Earth System Sciences*, *19*(3), 1521–1545. https://doi.org/10.5194/HESS-19-1521-2015

Smith, L. C., & Subandoro, A. (2007). Measuring food security using household expenditure surveys. *Food security in Practice technical guide series*. https://doi.org/10.2499/0896297675

Sternberg, T. (2012). Chinese drought, bread and the Arab Spring. *Applied Geography*, *34*, 519–524. https://doi.org/10.1016/j.apgeog.2012.02.004

Tadasse, G., Algieri, B., Kalkuhl, M., & von Braun, J. (2016). Drivers and triggers of international food price spikes and volatility. In K. Matthias, B. vonJoachim, & T. Maximo (Eds.), *Food price volatility and its implications for food security and policy* (pp. 59–82). Springer International Publishing. https://doi.org/10.1007/978-3-319-28201-5_3

Taylor, K. E., Stouffer, R. J., & Meehl, G. A. (2012). An overview of CMIP5 and the experiment design. *Bulletin of the American Meteorological Society*, *93*(4), 485–498. https://doi.org/10.1175/BAMS-D-11-00094.1

Thenkabail, P. S., Biradar, C. M., Noojipady, P., Dheeravath, V., Li, Y., Velpuri, M., et al. (2009). Global irrigated area map (GIAM), derived from remote sensing, for the end of the last millennium. *International Journal of Remote Sensing*, *30*(14), 3679–3733. https://doi.org/10.1080/01431160802698919

Tigchelaar, M., Battisti, D. S., Naylor, R. L., & Ray, D. (2018). K. Future warming increases probability of globally synchronized maize production shocks. *Proceedings of the National Academy of Sciences of the United States of America*, *115*(26), 6644–6649. https://doi.org/10.1073/pnas.1718031115

Trnka, M., Feng, S., Semenov, M. A., Olesen, J. E., Kersebaum, K. C., Rötter, R. P., et al. (2019). Mitigation efforts will not fully alleviate the increase in water scarcity occurrence probability in wheat-producing areas. *Science Advances*, *5*(9), eaau2406. https://doi.org/10.1126/sciadv.aau2406

Trnka, M., Meitner, J., Balek, J., Feng, S., Arbelaez Gaviria, J., Fischer, M., et al. (2025). Scientific data to paper -. Climate-induced severe water scarcity events as harbingers of global grain price [Dataset]. *ASEP Repository*. https://doi.org/10.57680/ASEP.0605406

Ubilava, D. (2017). The ENSO effect and asymmetries in wheat price dynamics. *World Development*, *96*, 490–502. https://doi.org/10.1016/j.worlddev.2017.03.031

Ubilava, D. (2018). The role of El Nino southern oscillation in commodity price movement and predictability. *American Journal of Agricultural Economics*, *100*(1), 239–263. https://doi.org/10.1093/ajae/aax060

Ubilava, D., & Abdolrahimi, M. (2019). The El Niño impact on maize yields is amplified in lower income teleconnected countries. *Environmental Research Letters*, *14*(5), 54008. https://doi.org/10.1088/1748-9326/ab0cd0

UN-Habitat, U. N. (2022). *United nations UN-Habitat world cities report - Envisaging the future of cities*. United Nations Human Settlements Programme (UN-Habitat).

van der Schrier, G., Efthymiadis, D., Briffa, K. R., & Jones, P. D. (2007). European Alpine moisture variability for 1800-2003. *International Journal of Climatology*, *27*(4), 415–427. https://doi.org/10.1002/JOC.1411

Van Meijl, H., Havlik, P., Lotze-Campen, H., Stehfest, E., Witzke, P., Domínguez, I. P., et al. (2018). Comparing impacts of climate change and mitigation on global agriculture by 2050. *Environmental Research Letters*, *13*(6), 064021. https://doi.org/10.1088/1748-9326/aabdc4

van Vuuren, D. P., Edmonds, J., Kainuma, M., Riahi, K., Thomson, A., Hibbard, K., et al. (2011). The representative concentration pathways: An overview. *Climatic Change*, *109*(1), 5–31. https://doi.org/10.1007/S10584-011-0148-Z/TABLES/4

Vicente-Serrano, S. M., Beguería, S., & López-Moreno, J. I. (2010). A multiscalar drought index sensitive to global warming: The standardized precipitation evapotranspiration index. *Journal of Climate*, *23*(7), 1696–1718. https://doi.org/10.1175/2009JCLI2909.1

Wang, Y., Bouri, E., Fareed, Z., & Dai, Y. (2022). Geopolitical risk and the systemic risk in the commodity markets under the war in Ukraine. *Finance Research Letters*, *49*, 103066. https://doi.org/10.1016/j.frl.2022.103066

World Bank Group. (2019). Special focus: Food price shocks: Channels and implications. In *Commodity markets outlook, April*. Retrieved from https://www.worldbank.org/commodities

World Bank Prospects Group. (2025). World bank commodity price data (the pink sheet). Retrieved from https://thedocs.worldbank.org/en/doc/18675f1d1639c7a34d463f59263ba0a2-0050012025/world-bank-commodities-price-data-the-pink-sheet

Zhu, P., Burney, J., Chang, J., Jin, Z., Mueller, N. D., Xin, Q., et al. (2022). Warming reduces global agricultural production by decreasing cropping frequency and yields. *Nature Climate Change 2022*, *12*(11), 1016–1023. https://doi.org/10.1038/s41558-022-01492-5